Enhancement and Inhibition of Coherent Phonon Emission of a Ni Film in a $BaTiO_3/SrTiO_3$ Cavity

N. D. Lanzillotti-Kimura,[1,2] A. Fainstein,[1] B. Perrin,[2] B. Jusserand,[2] A. Soukiassian,[3] X. X. Xi,[3,*] and D. G. Schlom[4]

[1]*Centro Atómico Bariloche and Instituto Balseiro, CNEA, 8400 San Carlos de Bariloche, Rio Negro, Argentina*

[2]*Institut des NanoSciences de Paris, UMR 7588 CNRS–Université Pierre et Marie Curie, 140 Rue de Lourmel, 75015 Paris, France*

[3]*Materials Research Institute, The Pennsylvania State University, University Park, Pennsylvania, 16802, USA*

[4]*Department of Materials Science and Engineering, Cornell University, Ithaca, New York, 14853-1501, USA*

(Received 20 November 2009; published 5 May 2010)

We report pump-probe time resolved reflectivity experiments in a hybrid air–Ni metal–$BaTiO_3/SrTiO_3$ oxide mirror phonon cavity. We demonstrate that the generated coherent acoustic phonon spectra of the impulsively excited metallic film can be inhibited or enhanced in the phonon cavity with respect to a Ni film directly grown on a $SrTiO_3$ substrate. The experiments are compared with simulations that highlight the role of the phonon density of states in the coherent acoustic emission, extending concepts at the base of the optical Purcell effect to the field of phononics.

DOI: 10.1103/PhysRevLett.104.187402 PACS numbers: 78.47.−p, 42.60.Da, 63.22.−m, 78.30.Fs

Changing the spontaneous light emission rate and spectra of atoms or excitons through the modification of the photon density of states (DOS) [1–4] has been the subject of significant efforts following Purcell's proposal and demonstration in the microwave domain [5]. Depending on the tuning of the emitter spectra with maxima or minima of the modified photonic DOS, the emission can be either enhanced or inhibited [3]. Similar ideas have been applied to modify other light-matter interaction processes [6–9]. In the field of phononics, and specifically the search of phonon ''lasing'' [10–12], for efficient monochromatic THz sources [11,13,14], and for the control of heat at the nanoscale, these ideas have not been pursued to date. Here we demonstrate that the coherent *acoustic phonon* emission spectra of an impulsively excited thin metallic film [15,16] can be either inhibited or enhanced by embedding the metal layer in an acoustic nanocavity [17]. This has been accomplished by using a hybrid metal cavity with a $BaTiO_3/SrTiO_3$ epitaxial oxide phonon mirror. Our results constitute the first necessary step to achieve full control of the emission rate of phonons in tailored materials.

Acoustic nanocavities [17–19] are the hypersound analog of optical microcavities. The latter have led, through the tailoring of the spatial and spectral confinement of the photon field, to optimized optical devices and novel physical phenomena [4,20]. Phonon cavities are constituted by acoustic mirrors enclosing a spacer of thickness equal to an integer number m of half-wavelengths ($m\lambda_{ac}/2$) [17]. The mirrors are made of stacks of repeated double layers of materials of contrasting acoustic impedance $Z = \rho v_{ac}$. Here ρ and v_{ac} are the material density and sound velocity, respectively. Such a resonator sustains confined modes, which can be designed to have perfect transmission in and out of the structure [17–19,21]. The cavity spacer in our experiments is made of an evaporated Ni thin film of nominal thickness $\approx$33 nm. The purpose of this investigation is to study the modification of the light-phonon transduction properties of this film induced by embedding it in a phonon cavity. We use a femtosecond laser light impulsion to generate a pulse of coherent sub-THz phonons in the metallic layer, and then we study how the latter is modified by changing the structure around the metal film. The essential idea is that the acoustic mirrors should not couple themselves with the light pulse and thus play no role in the phonon generation mechanism, except through the modification of the acoustic boundaries affecting the Ni emitter layer. We thus chose as the bottom broadband acoustic mirror a 10 period $BaTiO_3/SrTiO_3$ superlattice of thickness 64.6 Å/203.1 Å with the high-reflectivity stop band centered at $\approx$ 130 GHz [19,22]. $BaTiO_3$ and $SrTiO_3$ have optical energy gaps in the 350 nm range and are consequently completely transparent at the laser energy of 750 nm. Ni was chosen due to its acoustic impedance closely matching that of $SrTiO_3$ ($Z_{Ni} = 53.5$ and $Z_{SrTiO_3} = 40.9$, respectively). The sample-air interface responds to a free surface (zero-strain) boundary condition. This leads, ideally, to 100% acoustic reflectivity, and thus the surface performs as the top mirror to complete the phonon cavity. A schematic of the studied sample is shown in Fig. 1.

Figure 1 also displays in its top panel the surface displacement calculated using standard continuum matrix methods and assuming a white hypersound pulse impinging on the structure from the substrate. The calculation does not include attenuation, which could lead to a broadening of the cavity mode observed as a thin peak at $\sim$130 GHz. The bottom panel of Fig. 1 illustrates with an intensity graph the variation of the cavity response with spacer thickness. The thin band spanning the range from 140 GHz for a Ni thickness of 23 nm to $\sim$115 GHz for 43 nm describes the tuning of the cavity mode. The width of this curve is indicative of the change of cavity finesse (i.e., phonon lifetime) with mode detuning from the stop-band center. It follows that, due to the broadband mirrors used [19], the Ni metal layer thickness can be detuned by

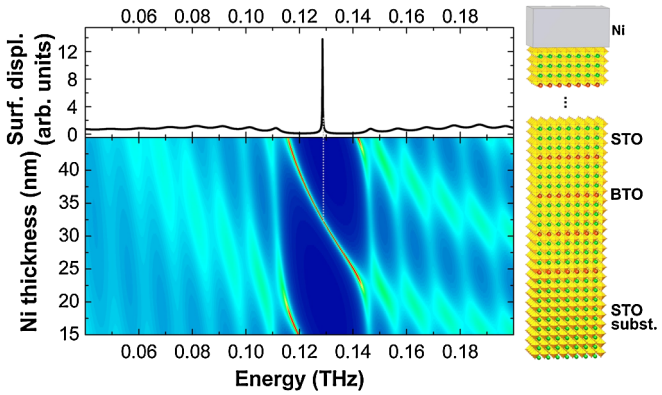

FIG. 1 (color online). Top: Calculated surface displacement of the hybrid metal-oxide cavity. Bottom: Intensity map of surface displacement versus Ni layer thickness. Inset: Schematic of the acoustic cavity structure. The number of unit cells does not correspond to the real structure. STO, $SrTiO_3$; BTO, $BaTiO_3$.

more than $\pm 30\%$ without significant broadening of the resonant cavity mode.

Room temperature reflection-type pump-probe experiments were performed at 750 nm with femtosecond laser pulses (≈ 80 fs) from a mode-locked Ti:sapphire laser. The measurements determine the real part of the change in the normalized reflectivity $\mathrm{Re}(\Delta r/r_0)$ induced on the metal layer by the acoustic phonons [15,16,23]. The left section of Fig. 2(a) shows $\mathrm{Re}(\Delta r/r_0)$, taken as a function of the time delay with respect to the pump pulse, on a test sample constituted by a Ni film deposited directly on a $SrTiO_3$ substrate (i.e., without the $BaTiO_3/SrTiO_3$ mirror). A broad signal related to the electronic response of the metal has been subtracted for clarity. At time zero an intense oscillation can be observed, which disappears within ~ 15 ps and is followed by clear single frequency oscillations that extend throughout the whole investigated time window. The intensity map in the right-hand panel of Fig. 2(a) displays the sliding Fourier transform of the time dependent reflectivity, obtained using 85 ps integration windows. The curve in this panel corresponds to the Fourier transform for the whole measured time scan. It is apparent from the peak at 50 GHz that the measured oscillations correspond almost exclusively to the Brillouin scattering of propagating acoustic waves in the $SrTiO_3$ substrate. The initial jump lasting ~ 15 ps displays a broad energy spectrum which is rapidly lost leaving its trace as weak bumps in the full-time Fourier transformed spectrum. It is due to the localized pulse generated and detected at the Ni layer, which rapidly escapes to the substrate facilitated by the acoustic impedance matching between the metal and $SrTiO_3$.

The situation is qualitatively modified when the $BaTiO_3/SrTiO_3$ mirror is added to form the acoustic cavity, as shown in Fig. 2(b). The coherent phonon time trace, displayed in the left-hand panel, now shows intense and complex higher frequency oscillations lasting 200 ps, followed by very weak stable oscillations. To analyze the

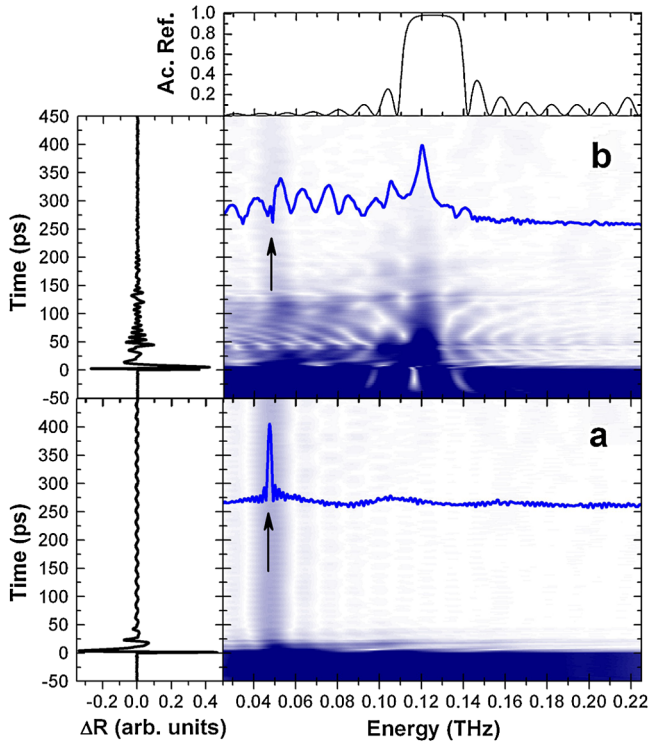

FIG. 2 (color online). Top panel: Acoustic reflectivity of the $BaTiO_3/SrTiO_3$ mirror. Left-hand panels: Time trace of $\mathrm{Re}(\Delta r/r_0)$. Right-hand panels: Sliding Fourier Transform calculated with 85 ps windows. The full Fourier spectrum is also included with thick curves. (a) Ni film deposited directly on $SrTiO_3$. (b) Hybrid metal-oxide acoustic cavity. The arrows indicate the Brillouin peak.

spectral content of the observed acoustic phonon signal, we show in the right-hand panel of Fig. 2(b) the sliding Fourier transform of the time trace, together with the full-time Fourier transform of $\mathrm{Re}(\Delta r/r_0)$. While a Brillouin component is still perceptible at all times (indicated with the vertical arrow), the spectral weight has been clearly transferred to higher energies. The most conspicuous feature is a peak located approximately at 120 GHz. The latter is characterized by an exponential decay with a time constant of ≈ 100 ps. Oscillations, particularly in the spectral range 0–100 GHz, can also be identified in the Fourier transform. To identify the relevant energy range, the top panel of Fig. 2(b) displays the calculated acoustic reflectivity of the $BaTiO_3/SrTiO_3$ mirror. Note that the intense peak at 120 GHz lies within the phonon stop band.

To evaluate the acoustic response of the structure we computed the phonon eigenstates of the system based on a continuum model with strain-free boundary conditions at the sample-air surface. The *generated spectrum* is calculated assuming that at time zero an ultrafast impulse defines a strain fully localized in the Ni layer. To characterize the *detection* properties of the device the time dependent change in reflectivity induced through a photoelastic mechanism in the Ni layer is evaluated [15,16]. We identify the peak at ~ 120 GHz in Fig. 2(b) as due to the cavity

confined mode. Thus, based on Fig. 1, we take the actual thickness of the evaporated Ni layer as 38.5 nm.

We first address the measured time dependent reflectivity traces shown in Fig. 2. Figure 3 presents the calculated position versus time strain intensity map. A scheme of the structure is also presented. As observed in Fig. 3, the escape time of the phonon pulse from the metal spacer layer is approximately ~15 ps. This time window determines the first intense feature observed in $\mathrm{Re}(\Delta r/r_0)$ for both the bare Ni and the hybrid-cavity structures (see Fig. 2). The establishment of a standing wave pattern is apparent in the cavity spacer after this first transient. These oscillations correspond to the cavity mode at ~120 GHz. The decay of the cavity-mode oscillation intensity with time is in part related to the tunneling of the phonons through the $BaTiO_3/SrTiO_3$ mirrors and into the substrate (observed in Fig. 3 at all times), and also to phonon lifetime decay which is not taken into account in the calculation. An additional secondary feature is the arrival at approximately 100 ps to the cavity spacer of a reflection of the initial pulse. This reflection is evidenced in the experimental $\mathrm{Re}(\Delta r/r_0)$ shown in Fig. 2(b) with a jump that adds to the cavity-mode related oscillations.

We now turn to the spectra of the generated coherent phonon signals. Figure 4 shows the calculated coherent phonon spectra generated by either the simple thin Ni layer deposited on the $SrTiO_3$ substrate (thick curve) or by the hybrid metal-oxide nanocavity (black thin curve). This figure also represents well the phonon spectrum extracted out of the Ni layer and transferred into the substrate. For comparison the actually measured phonon spectrum is also displayed. Several features are apparent. (i) The spectrum generated by the nonconfined Ni thin film is broad and almost featureless. It corresponds to the Fourier components of an acoustic pulse spatially localized within the film region. (ii) The spectrum emitted by the Ni film is qualitatively modified by the presence of the $BaTiO_3/SrTiO_3$ mirror. The most conspicuous feature is the strong enhancement of emission at the cavity mode (indicated by black color) and the inhibition within the stop band (gray shaded regions). (iii) Outside the phononic stop-band oscillations develop, which, when compared with the bare Ni-film, also express clear inhibition and enhancement regions. (iv) The experimental spectrum matches the calculation quite well. For the cavity structure there is a clear enhancement at the cavity mode, an indication of inhibition within the stop band, and oscillations with the appropriate period also denoting enhanced and reduced signal intensity with respect to the nonconfined structure. A broadening of the cavity mode and a reduced intensity of the higher energy phonons is also observed. These features possibly arise from phonon decay in the Ni layer, and a reduction of the metal-air interface reflectivity due to surface roughness [24].

To understand the origin of the observed change in generated spectrum, we recall the top panel of Fig. 1 showing the surface displacement of the hybrid metal-oxide cavity. This curve reflects the *local* acoustic DOS. In particular, within the phononic stop band modes are expelled and they concentrate at the cavity resonance and at the stop-band edges. It is this modification of the mode density landscape that determines at which energies acoustic phonons can be emitted by the metallic layer (enhancement at the cavity mode) and at which they cannot (inhibition within the phonon gap). A similar effect, though of smaller magnitude, leads to the observed oscillations in the coherent phonon generated spectra. These concepts are closely related to those at the base of "cavity quantum electrodynamics," the Purcell effect, and the search of light emission control by photon DOS engineering [1–7,9]. In fact, the spontaneous photon emission decay rate of an

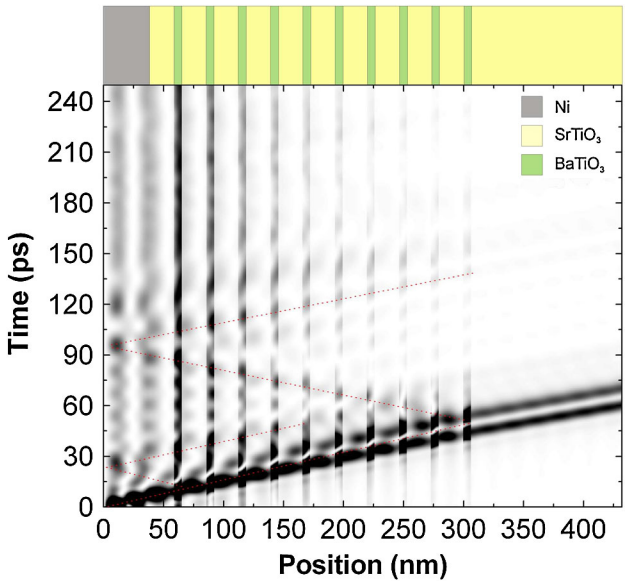

FIG. 3 (color online). Hypersound strain ($|du/dz|^2$) as a function of time for the hybrid-cavity structure. Dark regions correspond to larger stresses. No spectral filtering has been included. A scheme of the structure is shown at the top for comparison.

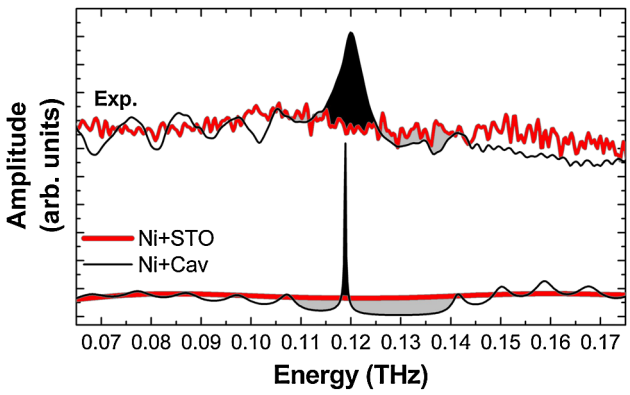

FIG. 4 (color online). Calculated (bottom) and measured (top) coherent phonon spectra generated by the thin Ni layer deposited on the $SrTiO_3$ substrate (thick curve) and by the hybrid metal-oxide nanocavity (black thin curve). Shaded black (gray) regions represent phonon emission enhancement (inhibition).

excited electronic state is also determined, through the Fermi golden rule, by the photon density of states at the emitter position [2]. The phononic effects described here are particularly strong because phonons are emitted normal to the layers and thus take maximum profit of the modified DOS. The equivalent quantum electrodynamic control on a single mode, or in a small aperture angle, has also been achieved for photons [6,7]. Controlling all photon modes so as to modify significantly the light emission rate is still a challenging problem in photonic devices [4]. Similarly, attaining full control of vibrational modes and thus of the emission rate of phonons emerges as a stimulating motivation with implications for the development of novel technologies, including phonon lasing [10–12].

In the experiment we report here we have a *spectrally broad* "emitter" (the ultrathin film which through photon-electron coupling leads to a localized perturbation of the strain field), and we demonstrate how the generation at some energies is enhanced and at others is inhibited. For the demonstration of the Purcell effect (i.e., the modification of the spontaneous phonon emission rate of an emitter induced by its environment) one would need to embed in a cavity a *spectrally narrow* emitter, energetically tuned to the cavity mode and spatially located at the position of the confined field (DOS amplitude) maximum [4]. Ruby might be a good candidate to demonstrate the phonon Purcell effect based on oxide cavities. Submicron thick ruby films can be evaporated with excellent quality for this purpose [25]. The Zeeman-split E(2E) Cr^{3+} doublet of ruby has long phonon-decay lifetimes in the sub-ms range, and a frequency that can be tuned from 1 to 5 cm^{-1} with external magnetic fields of reasonable magnitude (≤ 5 T) [12,25,26]. Such magnetic field would provide an external means by which it could be possible to tune the electron transition energy through that of the cavity confined mode. The mode lifetime (τ_{cav}) for a 1 cm^{-1} ruby cavity embedded between two symmetric $SrTiO_3/BaTiO_3$ mirrors could be varied from 300 ps to 150 ns by changing the number of mirror periods from 1 to 10. These lifetimes (corresponding to Q factors $Q = \omega/\Delta\omega$ that range from $\sim$10 to $\sim$4300) are much smaller than the phonon-decay lifetime of the Zeeman-split E(2E) Cr^{3+} doublet. This implies that the cavities would always be in the "weak-coupling regime" to which the Purcell effect belongs [4]. For a planar cavity, one could expect at most a Purcell enhancement factor for the *total* phonon emission rate of approximately 1.4, due to the penetration of the strain field in the distributed Bragg mirrors, and the coupling of the emitters to nonconfined modes over a large fraction of the total solid angle [27]. The phonon wavelengths involved ($\lambda_{phonon} \approx 240$ nm for 1 cm^{-1} phonons) would open the possibility, in addition, to laterally confine the phonon field by etching the planar cavity to form micropillars. The diameter for which the pillar would become better than the planar cavity for spontaneous phonon emission enhancement can be estimated to be around $d_{lim} \sim 20\lambda_{phonon} \sim 5$ μm [4]. The Purcell factor for a micropillar is $F_p = \frac{3}{4\pi^2}\frac{Q\lambda_{cav}}{LS}$, where L is the confined mode extension in the growth direction, $S \sim \pi d^2/16$ is the mode surface in the cavity plane, $\lambda_{cav}/L \sim 1/2$ for the Bragg mirrors used, and d is the pillar diameter [4]. For a 1 μm diameter micropillar, and a cavity Q factor = 1000, we estimate $F_p \sim 10$. Ruby should be held at liquid-helium temperatures to suppress transition between the Zeeman states that could obscure the Purcell effect [12,25,26].

In conclusion, we have demonstrated enhancement and inhibition of the generation of hypersound of a metal film impulsively excited by a laser pulse, using the modification of the local phonon density of states induced by embedding this film in an oxide mirror based cavity, and proposed a way to test the phonon Purcell effect in ruby. These ideas exploit in phononics fundamental concepts of cavity quantum electrodynamics.

*Current address: Department of Physics, Temple University, Philadelphia, PA 19122, USA.

[1] W. Lukosz and R. E. Kunz, J. Opt. Soc. Am. **67**, 1607 (1977).
[2] E. Snoeks *et al.*, Phys. Rev. Lett. **74**, 2459 (1995).
[3] E. Yablonovitch, Phys. Rev. Lett. **58**, 2059 (1987).
[4] See the tutorial on the Purcell effect by B. Gayral, Ann. Phys. (Paris) **26**, 1 (2001).
[5] E. Purcell, in *Proceedings of the American Physical Society, 1946* [Phys. Rev. 69, 681 (1946)].
[6] H.-B. Lin and A. J. Campillo, Phys. Rev. Lett. **73**, 2440 (1994).
[7] A. Fainstein *et al.*, Phys. Rev. B **53**, R13 287 (1996); A. Fainstein and B. Jusserand, Phys. Rev. B **57**, 2402 (1998).
[8] M. S. Kang *et al.*, Nature Phys. **5**, 276 (2009).
[9] Peter Bermel *et al.*, Phys. Rev. Lett. **99**, 053601 (2007).
[10] P. Hu, Phys. Rev. Lett. **44**, 417 (1980).
[11] A. J. Kent *et al.*, Phys. Rev. Lett. **96**, 215504 (2006).
[12] L. G. Tilstra *et al.*, Phys. Rev. B **76**, 024302 (2007).
[13] K.-H. Lin *et al.*, Nature Nanotech. **2**, 704 (2007).
[14] M. R. Armstrong *et al.*, Nature Phys. **5**, 285 (2009).
[15] C. Thomsen *et al.*, Phys. Rev. Lett. **53**, 989 (1984).
[16] O. Matsuda and O. B. Wright, J. Opt. Soc. Am. B **19**, 3028 (2002).
[17] M. Trigo *et al.*, Phys. Rev. Lett. **89**, 227402 (2002).
[18] A. Huynh *et al.*, Phys. Rev. Lett. **97**, 115502 (2006).
[19] A. Soukiassian *et al.*, Appl. Phys. Lett. **90**, 042909 (2007).
[20] J. Kasprzak, Nature (London) **443**, 409 (2006).
[21] Free membranes, as described by F. Hudert *et al.*, Phys. Rev. B **79**, 201307(R) (2009), also confine modes. However, these cannot couple with the outside.
[22] D. G. Schlom *et al.*, Mater. Sci. Eng. B **87**, 282 (2001).
[23] Similar results were obtained using a Sagnac interferometer. See B. Perrin *et al.*, Physica (Amsterdam) **219–220B**, 681 (1996).
[24] C.-L. Hsieh *et al.*, Appl. Phys. Lett. **85**, 4735 (2004).
[25] R. J. van Wijk *et al.*, J. Phys. Condens. Matter **3**, 3099 (1991).
[26] P. A. Fokker *et al.*, Phys. Rev. B **55**, 2925 (1997).
[27] A. M. Vredenberg *et al.*, Phys. Rev. Lett. **71**, 517 (1993).